Available online at www.sciencedirect.com
ScienceDirect
Earth and Planetary Science Letters 254 (2007) 28–38
EPSL
www.elsevier.com/locate/epsl

Postcollisional calc-alkaline lavas and xenoliths from the southern Qiangtang terrane, central Tibet

Lin Ding [a,*], Paul Kapp [b], Yahui Yue [a], Qingzhou Lai [a]

[a] *The Institute of Tibetan Plateau Research, and Institute of Geology and Geophysics, Chinese Academy of Sciences, Beijing, 100085, China*
[b] *Department of Geosciences, University of Arizona, Tucson, AZ 85721, USA*

Received 11 August 2006; received in revised form 10 November 2006; accepted 10 November 2006
Available online 22 December 2006
Editor: R.D. van der Hilst

Abstract

A newly recognized east–west trending province of 43 to 28 Ma volcanic rocks occurs in the southern Qiangtang terrane of central Tibet. The lavas are Na-rich calc-alkaline in composition, relatively primitive, and locally host ultramafic and mafic xenoliths. Foliated mafic granulite xenoliths from ~28 Ma lavas equilibrated at temperatures in the range of 980 to 1260 °C, indicating that the southern Qiangtang terrane lower crust was deformed and heated to very high temperatures during or before the Oligocene. In the northern Qiangtang terrane is a parallel suite of volcanic rocks of coeval age. However, here, the volcanic rocks are (ultra)potassic in composition and underlain by a hot (T>800 °C) metasedimentary-bearing lower crust. We suggest that both suites of Qiangtang lavas were derived from a primitive mantle source and that the enriched nature of the northern Qiangtang lavas reflects contamination by partial melts of metasedimentary lower crust. This contrasts with the conventional interpretation that Tibetan potassic lavas were solely derived from an ancient, enriched mantle lithospheric source. While removal of lithospheric mantle seems to be required to produce the high temperature melts, Eocene–Oligocene volcanism was coeval with thrust reactivation along bounding suture zones, implying that mantle dynamics were linked to intracontinental subduction.

Keywords: Tibetan plateau; Postcollisional volcanism; Xenoliths; Intracontinental subduction

1. Introduction

Much progress has been made in our understanding of the timing, distribution, and geochemistry of Tibetan postcollisional magmatism in recent years. Potassic volcanism initiated earlier than previously thought in both northern and southern Tibet (~25 Ma) and most notably in central Tibet where an east–west belt of 45 to 24 Ma (ultra)potassic volcanic rocks extends across the northern Qiangtang terrane (Fig. 1; [1,2]). A common interpretation is that Tibetan potassic magmas were derived from an ancient, enriched lithospheric mantle source that was heated following removal of lower parts of the lithospheric mantle [3–6]. However, high-temperature melting of granulitic or eclogitic lower crust can also produce partial melts of similar composition [7–9]. Xenoliths indicate unusually high temperatures (>800 °C) in the northern Tibetan lower crust [10,11] and geophysical results are widely

* Corresponding author. Tel.: +86 10 62849679; fax: +86 10 62849886.
E-mail address: dinglin@mail.igcas.ac.cn (L. Ding).

0012-821X/$ - see front matter © 2006 Elsevier B.V. All rights reserved.
doi:10.1016/j.epsl.2006.11.019

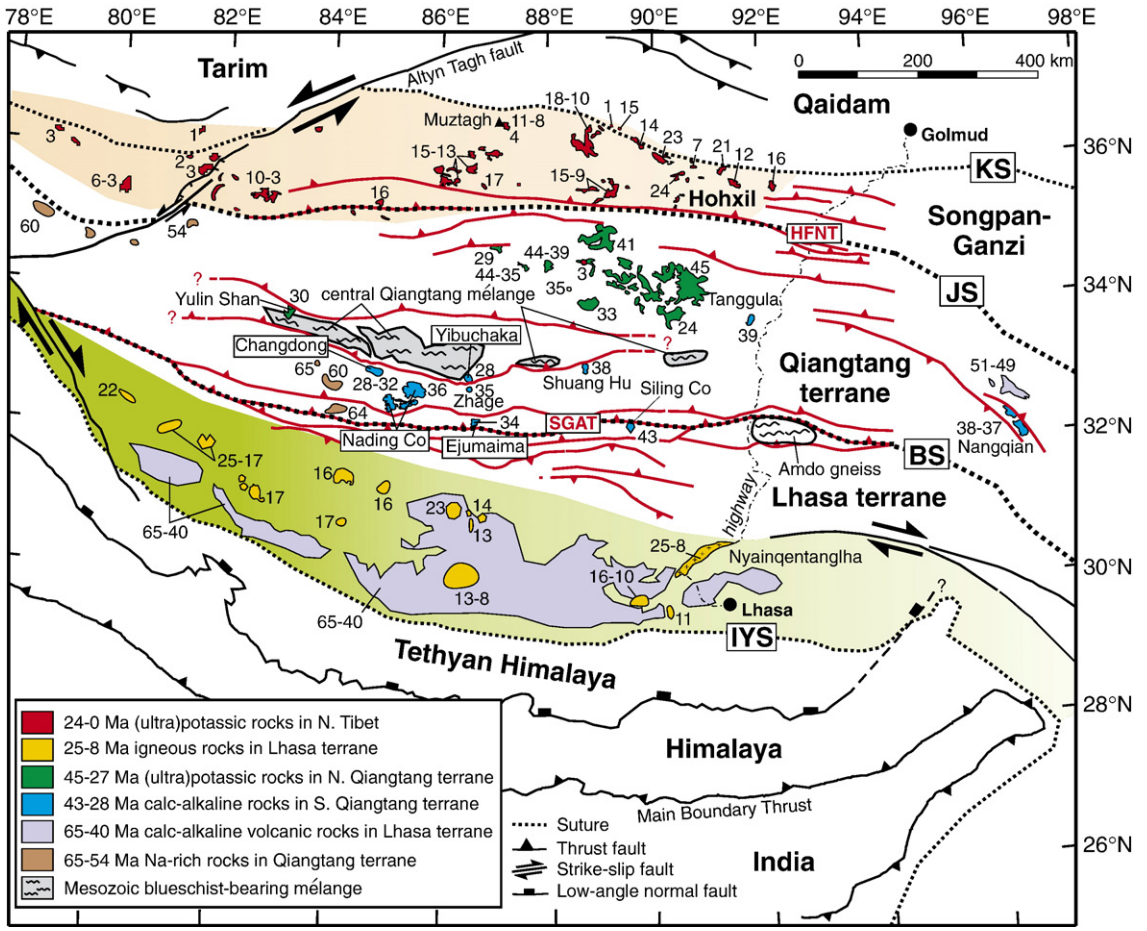

Fig. 1. Map of Tibet showing distribution of Cenozoic magmatism, Paleogene contractional structures (red; from [32]), and other major faults. The peach and green shading highlights belts of postcollisional volcanism to the north and south of the Qiangtang terrane, respectively. Ages are from [1] and references therein in addition to more recent studies [2,15,16,20,22,28,32–34]. Abbreviations: BS—Bangong suture; IYS—Indus–Yarlung suture; JS—Jinsha suture; KS—Kunlun suture; HFNT—Hohxil–Fenghuo Shan–Nangqian thrust belt; SGAT—Shiquanhe–Gaize–Amdo thrust belt.

interpreted to indicate that the middle and/or lower crust in southern Tibet includes zones of partial melt [12,13]. Recently discovered Miocene adakite-like rocks in both southern and northern Tibet likely reflect melts of mafic lower crust [14–16]. Also peculiar, are igneous rocks of Eocene–Oligocene age near Tanggula and Nangqian in east-central Tibet [17–20] and Miocene age near Lhasa [21,22] that have calc-alkaline compositions and isotopic affinities that are similar to those of precollisional igneous rocks in Tibet, including Linzizong volcanic rocks (~65 to 40 Ma) and the Gangdese batholith in southern Tibet (Fig. 1; [21,23–25]).

The newly recognized variability in Tibetan postcollisional magmatism has raised numerous contrasting tectonic models, many of which call upon some theme of continental subduction and mantle removal either acting in concert or at different times during the evolution of the Tibetan orogen [1,2,26–30]. At present, it seems that the only unequivocal tectonic requirements to produce Tibetan postcollisional magmatism are a heat source for melting and the presence of melt-fertile rocks. Hence, refinement of current models will continue to rely heavily on knowledge of the temporal–spatial–compositional distribution of postcollisional igneous rocks and its relationship to the style and timing of crustal deformation and lithospheric evolution as constrained by geological studies. Here, we present $^{40}Ar/^{39}Ar$, geochemical and Sr–Nd isotopic results that define an additional, previously unrecognized suite of postcollisional volcanic rocks in the southern Qiangtang terrane of central Tibet (Fig. 1). Furthermore, we document mafic and ultramafic xenoliths in these

rocks. In no other place within the plateau interior have ultramafic xenoliths been discovered within postcollisional lavas.

2. Southern Qiangtang volcanic rocks: geologic setting

The southern Qiangtang terrane is defined here to lie between the Jurassic–Cretaceous Bangong suture to the south and an east–west belt of Mesozoic blueschist-bearing metamorphic core complexes to the north (Fig. 1). Postcollisional volcanic rocks were first documented in the southern Qiangtang terrane near Nading Co (K–Ar age of ~31 Ma with no data table provided; [31]) and more recently near Siling Co (~43 Ma; [32]), Shuang Hu (~38 Ma; [33]), Zhage (~35 Ma [32]), and Changdong (28–32 Ma; [34]) (Fig. 1). In this study, we investigated postcollisional volcanic rocks near Nading Co and at two new localities: near Ejumaima to the south and Yibuchaka to the north (Fig. 1).

The Ejumaima volcanic rocks consist of sheeted lavas in four isolated monadnocks standing ~100 m above a surrounding pediplain and were erupted over an area of ~22 km^2. They are deformed by broad folds with ~1-km-scale wavelength and inferred to unconformably overlie more strongly deformed nonmarine red beds that are exposed ~5 km to the north in the footwall of a north-dipping thrust fault (Fig. 2). The Ejumaima volcanic rocks are characterized by gray sanidine-bearing trachytes in the lower part and black trachytes and vesicular trachyandesites in the upper part.

Volcanic rocks near Nading Co consist of lava sheets that were erupted over an area of >700 km^2, making this the largest documented volcanic field in the southern Qiangtang terrane. The lava sheets are generally subhorizontal, but locally shallow dipping toward the east in the proximal hanging walls of active west-dipping normal faults (Fig. 2). They unconformably overlie strongly folded Triassic marine and marginal marine strata and therefore postdate the bulk of upper crustal shortening in this area. The sheeted lavas generally consist of black hornblende-bearing basalt in the lower part and grey trachybasalt and trachyandesite in the upper part. One locality was identified where basalt flows host numerous ultramafic xenoliths.

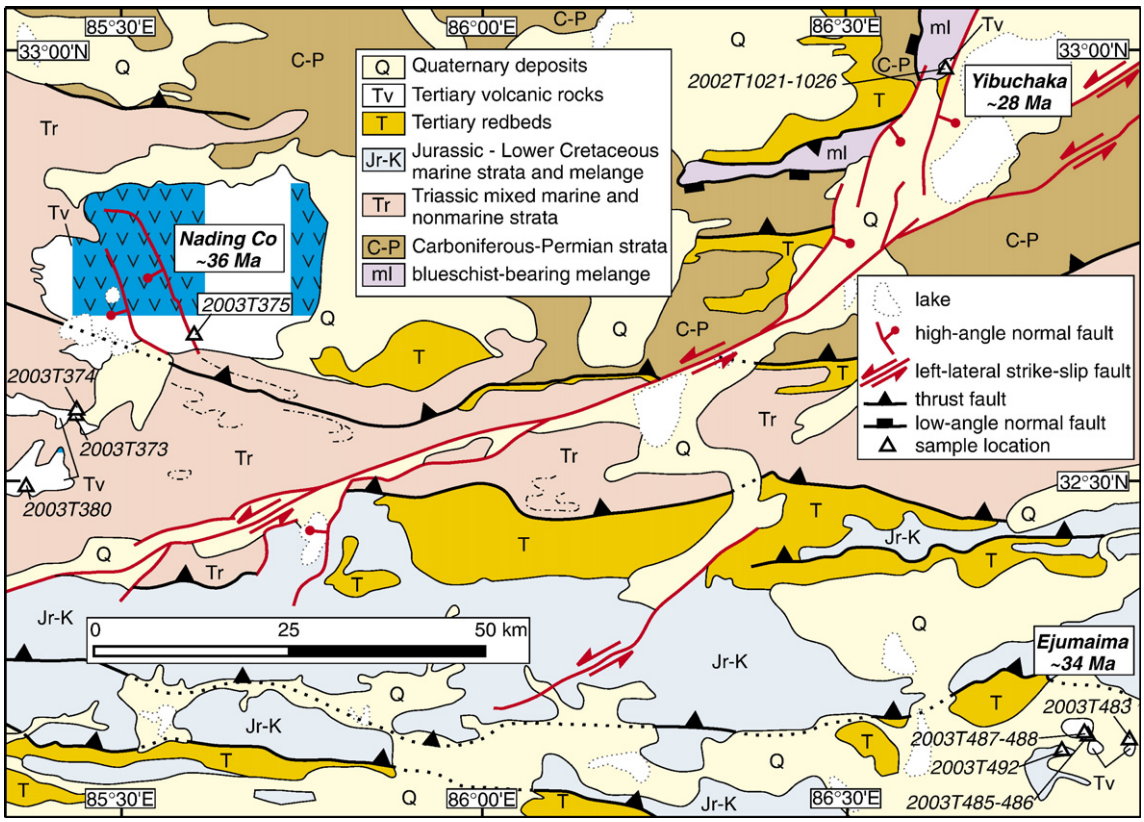

Fig. 2. Geologic map of the south-central Qiangtang terrane based on [32] and our more recent mapping and analysis of satellite imagery.

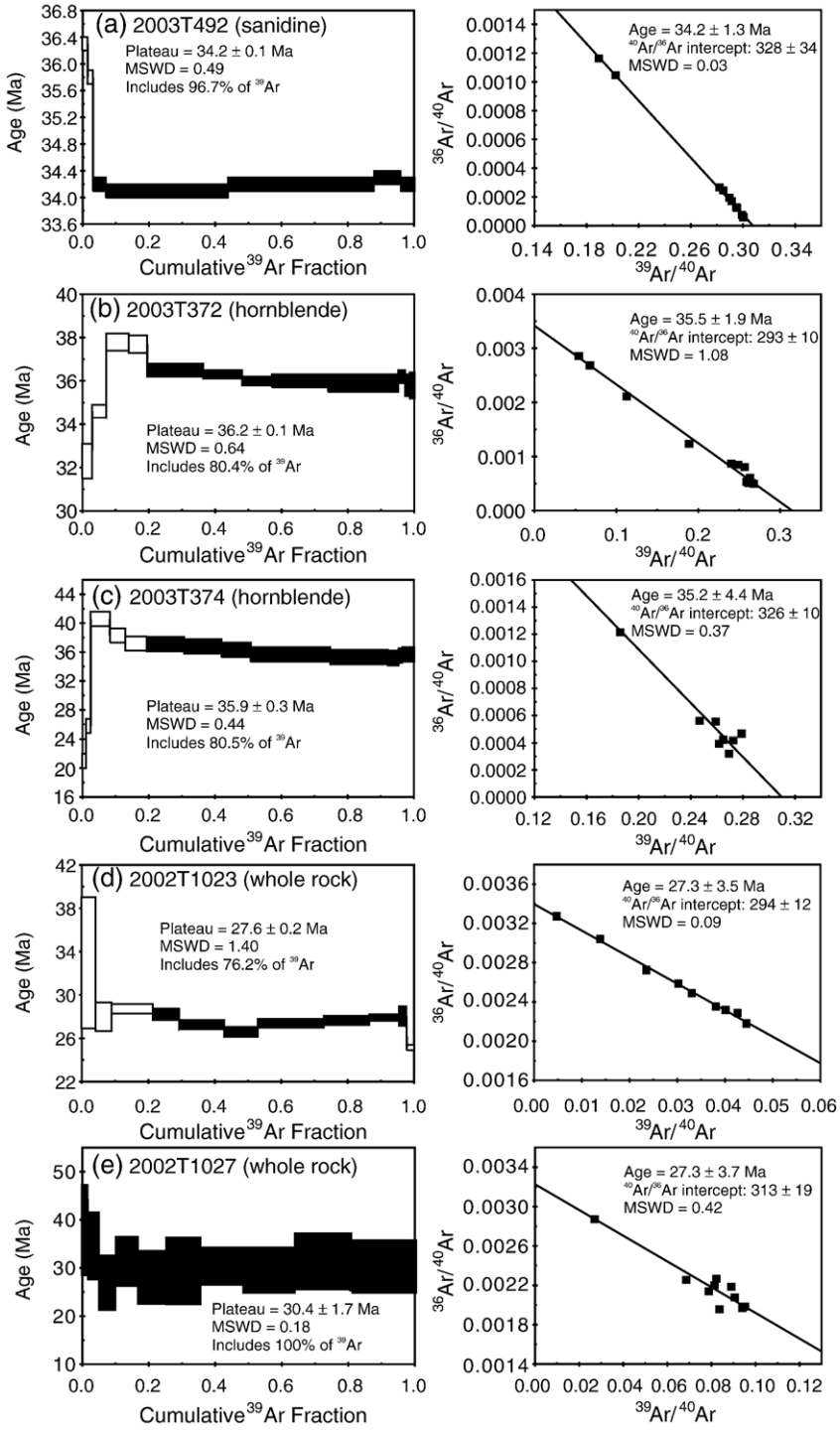

Fig. 3. Argon age spectra and inverse isochron plots.

On the west side of Yibuchaka lake (Fig. 2) near the village of Rongma, lake terraces are cut into a relatively small exposure (~3 km^2) of black, massive trachyandesites that host numerous ultramafic and mafic xenoliths. The volcanic rocks occur within an active system of east-dipping normal faults [35] and are locally unconformably overlain by Quaternary lake terrace sediments.

3. Geochronology

$^{40}Ar/^{39}Ar$ analyses were conducted on five samples from the Ejumaima, Nading Co, and Yibuchaka areas. Analytical procedures followed those described in [36]. Mineral (hornblende or sanidine) and whole-rock separates were irradiated for 36 h at the Beijing Nuclear Research Institute Reactor. Also irradiated was Fish Canyon sanidine (28.2 Ma) to calculate J factors and K_2S0_4 and CaF_2 to determine correction factors for interfering neutron reactions. All samples were step heated using a radiofrequency furnace. Argon isotope analyses were conducted on a VG 5400 mass spectrometer in the Laboratory of Isotope Geochronology at the Institute of Geology and Geophysics, Chinese Academy of Sciences (IGGCAS). Blanks were measured before each sample analysis with typical background values for ^{40}Ar, ^{39}Ar, ^{37}Ar and ^{36}Ar of 2.44×10^{-14}, 5.82×10^{-16}, 4.61×10^{-16} and 5.43×10^{-16} mol, respectively. The interlaboratory correction factors at the time of the analysis were as follows: $(^{36}Ar/^{37}Ar)_{Ca}=2.64\times10^{-4}$, $(^{40}Ar/^{39}Ar)_K=3.05\times10^{-2}$, $(^{39}Ar/^{37}Ar)_{Ca}=6.87\times10^{-4}$, $(^{38}Ar/^{39}Ar)_K=0.01$, $(^{37}Ar/^{38}Ar)_{Ca}=3.81\times10^{-5}$, $(^{38}Ar/^{36}Ar)a=0.1869$, $(^{40}Ar/^{36}Ar)a=294.1$, $(^{36}Ar/^{38}Ar)_{Cl}=4.35\times10^{-4}$. Age calculations were made using the total decay constant of $(5.543\pm0.010)\times10^{-10}a^{-1}$ given in [37]. The cited age uncertainties are at the 1σ level and include uncertainties in J and the total decay constant. A complete data table is provided in supplementary material (Table A1) whereas age spectra and isochron plots are shown in Fig. 3.

$^{40}Ar/^{39}Ar$ plateau ages are interpreted to provide eruption ages for the samples; all of the plateau ages are well defined over ≥75% cumulative ^{39}Ar released and statistically indistinguishable from their corresponding inverse isochron ages (Fig. 3). Sanidine phenocrysts from a sample near the base of the Ejumaima lava sheets (2003T492) yielded a plateau age of 34.2±0.1 Ma. Hornblende phenocrysts from two Nading Co basaltic lavas (2003T372 and 2003T374) yielded plateau ages of 36.2±0.1 Ma and 35.9±0.3 Ma, respectively. Two whole rock samples of Yibuchaka basalt (2002T1023 and 2002T1027) yielded plateau ages of 27.6±0.2 Ma and 30.4±1.7 Ma, respectively.

Integration of previous geochronology with these new results suggests that southern Qiangtang volcanism was active between 43 and 27 Ma. These ages are similar to that of an east–west belt of (ultra)potassic volcanic rocks in the northern Qiangtang terrane (45–24 Ma) and calc-alkaline igneous rocks along strike to the east near Tanggula and Nangqian (Fig. 1 and references in the caption). Furthermore, potassic volcanic rocks of this age are distributed along the Batang–Lijiang and Red River fault systems in eastern Tibet and Indochina (42–24 Ma; [6,38]).

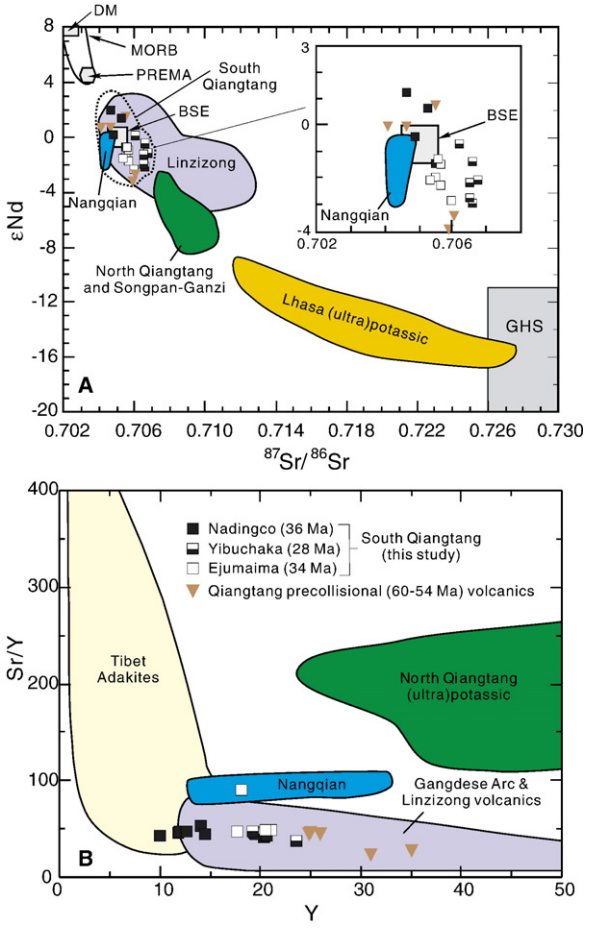

Fig. 4. Plots of A: Initial εNd vs. $^{87}Sr/^{86}Sr$ and B: Sr/Y vs. Y. Fields for Tibetan adakites and the calc-alkaline Gangdese Arc are taken from [14]. Other data sources are same as in Fig. 1.

4. Geochemistry

Major and trace element and Sr–Nd isotopic data from 16 whole rock samples from the Ejumaima ($n=6$), Nading Co ($n=4$), and Yibuchaka ($n=6$) areas were obtained at the IGGCAS and are tabulated in the supplementary material (Tables A2 and A3). Major element abundances (wt.%) were determined on whole-rock powder pellets by an XRF-1500 sequential X-ray fluorescence spectrometer. Analytical uncertainties are 1 to 3% for major elements. Rare earth element (REE) and trace element analyses were determined by a PQ2 Turbo inductively coupled plasma mass spectrometer. Uncertainties, in ppm, based on repeated

analyses of internal standards, are ±5% for REE and ~5–10% for trace elements. Rb–Sr and Sm–Nd isotopic analyses were conducted on a VG354 mass spectrometer. Within-run isotope fractionation was corrected for using $^{146}Nd/^{144}Nd=0.7219$ and $^{86}Sr/^{88}Sr=0.1194$. Eight analyses of the NBS987 Sr standard ($^{86}Sr/^{88}Sr=0.710240$) yielded an average $^{86}Sr/^{88}Sr$ value of 0.710254±0.000014, and 12 analyses of the La Jolla Nd standard ($^{143}Nd/^{144}Nd=0.511859$) yielded an $^{143}Nd/^{144}Nd$ average value of 0.511862±0.000007. Analytical precision of isotope ratio measurement is given as 2σ.

The southern Qiangtang magmas are characterized by mafic to felsic calc-alkaline compositions (SiO_2 contents range from ~47 to 67 wt.%). They are sodium rich (Na_2O contents up to 4.5 wt.% with K_2O/Na_2O generally <1), distinguishing them from the postcollisional belts of (ultra)potassic rocks to the north and

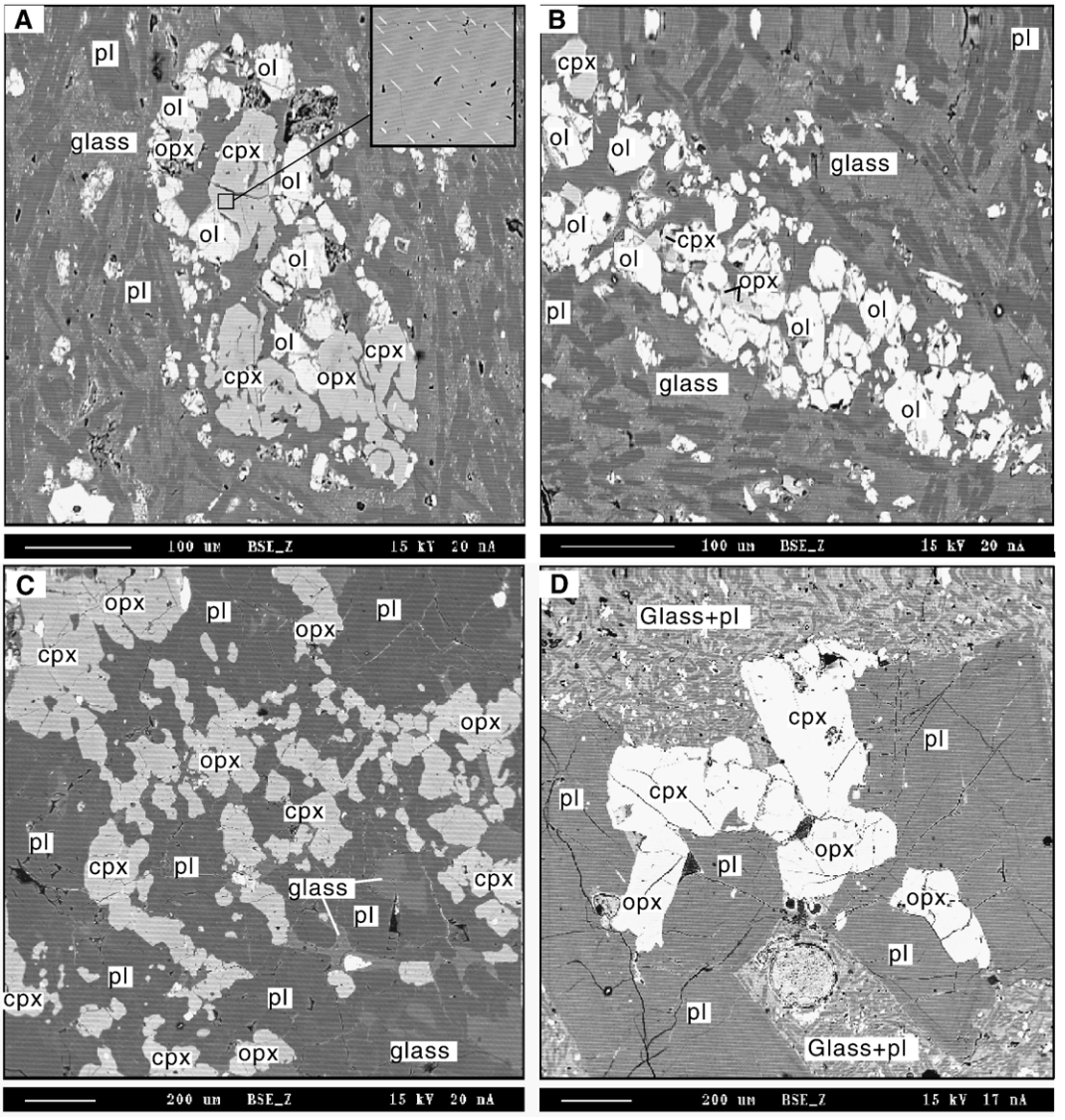

Fig. 5. Backscattered electron images showing the textures of xenoliths from the Yibuchaka volcanic rocks. Mineral abbreviations: cpx—clinopyroxene, ol—olivine; opx—orthopyroxene; pl—plagioclase, A: Olivine websterite in sample 2002T102-2. The xenolith fractures are filled by volcanic glass. The volcanic groundmass consists of plagioclase laths (dark gray) and glass (light gray). Insert shows clinopyroxene with exsolution rods of rutile. B: Lherzolite in sample 2002T102-3. C: Granulite in sample 2002T102-3. D: Granulite in sample 2002T102-4. Note the shape-preferred orientation of minerals in xenoliths shown in A–C.

south [1,2,5], the high-K calc-alkaline rocks in the Nangqian region [20], and the northern Tibetan K-rich adakites [16]. The initial $^{87}Sr/^{86}Sr$ (0.704–0.706) and $^{143}Nd/^{144}Nd$ (0.5124–0.5128) values of the southern Qiangtang volcanic rocks are similar to those of Lhasa terrane adakites [14,15] and precollisional Na-rich lavas in the Qiangtang terrane (60–54 Ma; [1]) and Linzizong calc-alkaline volcanic rocks [11] (Fig. 4A). However, southern Qiangtang lavas differ from Linzizong volcanic rocks by their higher Sr contents (400–1600 ppm) and lower Y contents (10–21 ppm) and from Lhasa terrane adakites by lower Sr/Y values, higher Y contents (Fig. 4B), and higher MgO contents. On the basis of these comparisons, we conclude that the southern Qiangtang lavas represent a newly discovered, geochemically distinct suite of postcollisional magmatism in Tibet.

5. Xenoliths

Xenoliths in the Yibuchaka lavas were investigated in this study. The xenoliths are relatively small, ranging in size from 0.1 cm to 0.5 cm in diameter. Two types of xenoliths were identified: ultramafic and mafic granulite. The ultramafic xenoliths consist of clinopyroxene + orthopyroxene (websterites) and olivine + clinopyroxene + orthopyroxene ± spinel (lherzolites and olivine websterites). The modal proportion of olivine is highly variable in the latter, ranging from <50% to ~90%. The olivine-bearing xenoliths exhibit a foliation defined by oblate pyroxene and olivine grains (Fig. 5A and B). The mafic granulite xenoliths consist of clinopyroxene + orthopyroxene + plagioclase. Most of these xenoliths show a weak foliation defined by a shape-preferred mineral orientation (Fig. 5C), although some of the xenoliths are comprised of euhedral minerals without a preferred orientation (Fig. 5D).

Compositions of minerals in 13 xenolith samples were determined using a CAMECA SX51 electron microprobe at IGGCAS. The accelerating voltage was 21 kV, the sample current was 10 nA, and beam diameter was 1 μm. Counting times for all elements were 10 s. Pre-eruption xenolith temperatures were determined by using the two-pyroxene thermometer of [39] and core compositions of coexisting orthopyroxene and clinopyroxene. Mineral compositional data, along with thermometric results for individual xenoliths, are provided as supplementary information (Table A4). The olivine-bearing, websterite, and mafic granulite xenoliths yield mean temperatures of 1044 ± 43 °C, 1076 ± 96 °C, and ~980 °C, respectively. At these temperatures, the absence of garnet provides maximum pressure estimates of ~1.7–1.8 GPa for the olivine-bearing xenoliths and ~1.3–1.4 GPa for the websterite and mafic granulite xenoliths [40].

Physical properties of the xenoliths were estimated using the methodology described in [41] and are provided in Table A5. Input parameters included mineral volume proportions estimated from backscattered electron images, the mineral compositional data and calculated pre-eruption temperatures, and a fixed pressure of 1 GPa. We note that varying pressures over a feasible range at a given temperature yields minimal variations (<5%) in the calculated physical properties. Estimated *P*-wave speeds for the olivine-bearing, websterite, and mafic granulite xenoliths are 7.36 ± .07 km/s, 7.17 ± 0.08 km/s, and ~6.6 km/s, respectively. Poisson's ratios for the olivine-bearing, websterite, and mafic granulite range from 0.27–0.29, 0.25–0.26, and 0.28–0.29, respectively. Collectively, the xenoliths yield Poisson's ratios that are very similar to, but *P*-wave speeds that are significantly lower, than those determined experimentally for similar lithologies at 1 GPa [42].

6. Discussion and conclusions

6.1. Xenoliths

The olivine-bearing xenoliths were likely entrained from the upper continental mantle lithosphere. The absence or very thin (<5 μm) compositional zonation of the olivine along with the absence of olivine phenocrysts in the matrix suggest that these xenoliths did not crystallize from a host melt. The unusually low magnesium olivine (forsterite contents of 65–70 wt.%) and slow *P*-wave speeds (~7.36 km/s) of the olivine-bearing xenoliths suggest that they do not represent typical mantle rocks olivine with forsterite contents >90 wt.% and *P*-wave speeds >7.7 km/s) but rather low-magnesium, fertile peridotite. In contrast, the maximum pressure estimates of ~1.3–1.4 GPa and P-wave speeds for the websterite (~7.17 km/s) and mafic granulite (~6.6 km/s) xenoliths suggest that they were entrained from the lowermost crust (or crust–mantle transition boundary) and lower crust, respectively. The presence of low magnesium rocks in the upper mantle and the unusually low seismic wave speeds of the ultramafic and mafic granulite xenoliths are consistent with the low seismic velocity and complexity of the Moho transition that has been observed in this region [43,44]. Furthermore, the foliated nature of the xenoliths implies that the lower crust and upper mantle of the southern Qiangtang terrane were penetratively deformed

prior to ~28 Ma. This finding urges caution in the common practice of assuming that observed seismic anisotropy in Tibet is a reflection of present-day deformation.

Thermometry of the websterite and mafic granulite xenoliths suggests that the lower crust of the southern Qiangtang terrane reached very high temperatures (≥980 °C) at or by ~28 Ma. The xenoliths were likely heated as they were entrained into the melt. However, consideration of the short timescales for magma ascent and the relatively slow rate of volume diffusion in pyroxene suggest that the calculated temperatures are unlikely a reflection of this transient heating event [9]. The recognition of a very hot Tibetan lower crust is not new. Studies of lower crustal xenoliths in the northern Qiangtang terrane [10] and near the Kunlun fault in northern Tibet [11] suggest similarly high lower crustal temperatures. However, the latter studies were conducted on xenoliths from mid-Miocene and younger lavas. Hence, this study is the first to show that anomalously high lower crustal temperatures were established in central Tibet as early as the Late Oligocene. Whether this is suggestive of a distinct heating event or, alternatively, that the lower crust of Tibet has been anomalously hot for at least the past 28 Myr, requires additional information.

6.2. Tectonic model

An intriguing question raised by this study is why are there parallel, east–west trending suites of volcanic rocks in the Qiangtang terrane that are coeval (Eocene–Oligocene) but exhibit contrasting geochemical characteristics (Na-rich calc-alkaline in the south; ultrapotassic to potassic in the north). Results of xenolith studies, albeit scarce and incomplete, are consistent with the two regions having experienced a similar thermal evolution. Both regions shared a similar structural setting during the Eocene–Oligocene. The northern Qiangtang lavas are located south of the Paleogene Hohxil–Fenghuo Shan–Nanqian thrust belt (Figs. 1 and 6), which is superimposed on the Triassic–Jurassic Jinsha suture zone and is estimated to have accommodated >40–50% shortening during the early Tertiary [20,45]. The southern Qiangtang volcanic suite is located north of the Jurassic–Cretaceous Bangong suture zone, which was substantially modified by the Tertiary north-dipping Shiquanhe–Gaize–Amdo thrust system [32,46] (Fig. 1). The Qiangtang terrane interior also underwent internal shortening coeval with volcanism (Figs. 1 and 6), but to a lesser extent than its bounding suture zones [32,45]. The only significant, recognized difference between the northern and southern Qiangtang terrane is the composition of the lower crust, discussed below.

The southern Qiangtang magmas are geochemically and isotopically similar to precollisional igneous rocks in Tibet (Fig. 4A and B). From this, we infer they were derived from a relatively juvenile mantle source of Asian affinity with intra-suite geochemical variations being explained by variable degrees of fractional crystallization and assimilation of lower crustal mafic rocks. Following the conventional interpretation that Tibetan potassic magmas were derived from an ancient and enriched mantle source [5], the dichotomy of Qiangtang magmatism would demand an extreme north–south variation in the nature of the Qiangtang mantle (with the northern Qiangtang mantle being ancient and enriched). However, the northern Qiangtang mantle is inferred to have been completely removed by

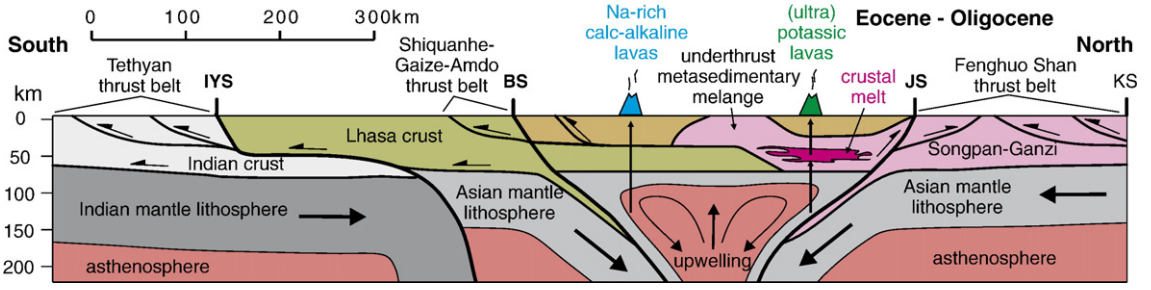

Fig. 6. Schematic lithosphere-scale cross section of Tibet during the Eocene–Oligocene. Geologic arguments supporting the crustal structure shown are provided in [20,26,32,46,48]. India's northward insertion into Tibet drives intracontinental subduction beneath the Qiangtang terrane along reactivated suture zones. Upwelling of asthenosphere beneath central Tibet, induced by intracontinental subduction, produces a heat source for magmatism. Qiangtang lavas are derived from an Asian mantle source. The potassic nature of northern Qiangtang lavas is due to mixing of mantle melts with partial melts of metasedimentary-bearing lower crust. Abbreviations: BS—Bangong suture; IYS—Indus–Yarlung suture; JS—Jinsha suture; KS—Kunlun suture.

Mesozoic southward low-angle oceanic subduction along the Jinsha suture to the north, during which Songpan–Ganzi sedimentary rocks and metasedimentary-matrix mélange underthrust Qiangtang continental margin rocks [47,48]. This hypothesis explains the exhumed belt of blueschist-bearing mélange within the middle of the Qiangtang terrane, hundreds of kilometers south of the Jinsha suture, and which at present separates the two contrasting volcanic suites (Fig. 1). Importantly, it predicts that the northern Qiangtang terrane is underlain by a metasedimentary-bearing lower crust (Fig. 1). Although not proving the hypothesis, this prediction has been directly validated through documentation of metasedimentary lower crustal xenoliths in northern Qiangtang lavas [10].

In contrast, strata of the southern Qiangtang terrane are likely underlain by crystalline basement and a dominantly mafic lower crust. Based on wide-angle seismic profiles, a high-velocity layer in the lower crust characteristic of mafic rocks is present in the southern Qiangtang terrane [49] but absent in the northern Qiangtang terrane [50]. Major Cretaceous–early Tertiary south-directed thrusting in the Lhasa terrane and coeval growth of a major antiformal culmination in the central Qiangtang terrane have been attributed to large-scale northward underthrusting of Lhasa terrane crystalline basement beneath the Qiangtang terrane [32,46,51]. Furthermore, Cambrian and older orthogneisses in the Amdo area along the Bangong suture (Fig. 1) have recently been suggested to represent exhumed portions of southern Qiangtang terrane basement [52].

Given that the only notable difference between the northern and southern Qiangtang terrane is lower crustal composition, we call on this difference to explain the contrasting geochemistry of the two volcanic suites. We suggest that the northern Qiangtang lavas were derived from a relatively juvenile mantle source, similar to the southern Qiangtang lavas, and that their potassic nature is a consequence of mixing with partial melt of metasedimentary-bearing lower crust (Fig. 6). This hypothesis bears similarity to a recent proposal by [30], showing through trace element modeling that Tibetan potassic magmatism can be explained by partial melt of an asthenospheric source enriched by sediment subducted along with Indian lithosphere. However, Indian lithosphere is predicted to have underthrust only as far north as the Indus–Yarlung suture by ~45 Ma [26], when potassic magmatism commenced in the northern Qiangtang terrane. Furthermore, our comparison between the northern and southern Qiangtang terrane suggests that enrichment, at least in this region, occurred by mixing with partial melt in the lower crust. While our hypothesis is most convincingly argued for central Tibet, the sources of other potassic lavas in northern, southern, and eastern Tibet also could include melts of supracrustal rocks that were introduced into the Tibetan lower crust (and possibly mantle as in the Pamir [9,53] and also suggested for Tibet [1,30,38]) by continental underthrusting/subduction during the Indo–Asian collision. Left unexplained is the tectonic process by which the high-temperatures necessary for melt production was achieved in central Tibet during the Eocene–Oligocene. Convective removal of thickened continental mantle lithosphere [4,5] could explain the thermal perturbation. However, given that Eocene–Oligocene volcanism in Tibet is restricted in location between the suture zones bounding the Qiangtang terrane (Fig. 1), and was contemporaneous with major reactivation of these suture zones during the Tertiary, we favor a model in which heat advection in the mantle was driven by intracontinental subduction (Fig. 6) [1,18,30,54].

7. Conclusions

This study identifies an east–west trending suite of Eocene–Oligocene calc-alkaline volcanic rocks in the southern Qiangtang terrane of central Tibet that contrasts in geochemistry with a parallel and coeval suite of (ultra)potassic volcanic rocks in the northern Qiangtang terrane. There is compelling evidence that the northern suite is underlain by a metasedimentary-bearing lower crust whereas the southern suite is underlain by crystalline basement and a mafic lower crust. A simple petrogenetic explanation is that both suites of volcanic rocks were derived from relatively juvenile mantle sources, with the potassic nature of the northern lavas being due to mixing with partial melts of metasedimentary-bearing lower crust. Previous studies of xenoliths in mid-Miocene and younger lavas have detected anomalously hot temperatures in the Tibetan lower crust. Our study of mafic and ultramafic xenoliths in southern Qiangtang lavas suggests that such high temperatures were achieved in the central Tibetan lower crust during or before the Oligocene.

Acknowledgments

We thank F.K. Chen, H. Sang, H. Li, X.D. Jin. and Y. Ma for their assistance with laboratory analyses, Michael Edwards and Marc Jolivet for their comments on an earlier version of this manuscript, and Bradley Hacker and An Yin for their constructive reviews. This work was supported by grants from the Chinese Academy of Sciences (KZCX3-SW-143 to Ding), Chinese Ministry

of Science and Technology (2002CB412602 to Ding), National Natural Science Foundation of China (40625008 to Ding), U.S. National Science Foundation (EAR-0309844 and EAR-0438120 to Kapp), and National Geographic Society (#7841-05 to Kapp).

Appendix A. Supplementary data

Supplementary data associated with this article can be found, in the online version, at doi:10.1016/j.epsl.2006.11.019.

References

[1] L. Ding, P. Kapp, D. Zhong, W. Deng, Cenozoic volcanism in Tibet: evidence for a transition from oceanic to continental subduction, J. Petrol. 44 (2003) 1833–1865.

[2] S.-L. Chung, M.-F. Chu, Y. Zhang, Y. Xie, C.-H. Lo, T.-Y. Lee, C.-Y. Lan, X. Li, Q. Zhang, Y. Wang, Tibetan tectonic evolution inferred from spatial and temporal variations in post-collisional magmatism, Earth-Sci. Rev. 68 (2005) 173–196.

[3] S. Turner, C. Hawkesworth, J. Liu, N. Rogers, S. Kelley, P. Calsteren, Timing of Tibetan uplift constrained by analysis of volcanic rocks, Nature 364 (1993) 50–54.

[4] P. Molnar, P. England, J. Martinod, Mantle dynamics, uplift of the Tibetan Plateau, and the India monsoon, Rev. Geophys. 31 (1993) 357–396.

[5] S. Turner, N. Arnaud, J. Liu, N. Rogers, C. Hawkesworth, N. Harris, S. Kelley, P. Van Calsteren, W. Deng, Post-collision, shoshonitic volcanism on the Tibetan plateau: implications for convective thinning of the lithosphere and the source of ocean island basalts, J. Petrol. 37 (1996) 45–71.

[6] S.-L. Chung, C.-H. Lo, T.-Y. Lee, Y. Zhang, Y. Xie, X. Li, K.-L. Wang, P.L., Diachronous uplift of the Tibetan plateau starting 40 Myr ago, Nature 394 (1998) 769–773.

[7] A.E. Patiño Douce, T.C. McCarthy, Melting of crustal rocks during continental collision and subduction, in: B.R. Hacker, J.G. Liou (Eds.), When Continents Colllide: Geodynamics and Geochemistry of Ultrahigh-Pressure Rocks, Kluwer Academic Publishers, Dordrecht, 1998, pp. 27–55.

[8] K.M. Cooper, M.R. Reid, N.W. Dunbar, W.C. McIntosh, Origin of mafic magmas beneath northwestern Tibet: constraints from 230Th–238U disequilibria, Geochem., Geophys., Geosyst. 3 (2002), doi:10.1029/2002GC000332.

[9] B. Hacker, P. Luffi, V. Lutkov, V.T. Minaev, L. Ratschbacher, T. Plank, M. Ducea, A. Patiño-Douce, M. McWilliams, J. Metcalf, Near-ultrahigh pressure processing of continental crust: Miocene crustal xenoliths from the Pamir, J. Petrol. 46 (2005) 1661–1687.

[10] B.R. Hacker, E. Gnos, L. Ratschbacher, M. Grove, M. McWilliams, S.V. Sobolev, J. Wan, W. Zhenhan, Hot and dry deep crustal xenoliths from Tibet, Science 287 (2000) 2463–2466.

[11] M. Jolivet, M. Brunel, D. Seward, Z. Xu, J. Yang, J. Malavieille, F. Roger, A. Leyreloup, N. Arnaud, C. Wu, Neogene extension and volcanism in the Kunlun Fault Zone, northern Tibet: new constraints on the age of the Kunlun Fault, Tectonics 22 (2003) 1052, doi:10.1029/2002TC001428.

[12] K.D. Nelson, W. Zhao, L.D. Brown, J. Kuo, J. Che, X. Liu, S.L. Klemperer, Y. Makovsky, R. Meissner, J. Mechie, R. Kind, F. Wenzel, J. Ni, J. Nabelek, Leshou Chen, H. Tan, W. Wei, A.G. Jones, J. Booker, M. Unsworth, W.S.F. Kidd, M. Hauck, D. Alsdorf, A. Ross, M. Cogan, C. Wu, E. Sandvol, M. Edwards, Partially molten middle crust beneath southern Tibet: synthesis of Project INDEPTH results, Nature 274 (1996) 1684–1688.

[13] S.L. Klemperer, Crustal flow in Tibet: A review of geophysical evidence for the physical state of Tibetan lithosphere, in: M.P. Searle, R.D. Law, L. Godin (Eds.), Channel flow, ductile extrusion and exhumation of lower mid-crust in continental collision zones Special Publication, Geological Society of London, London, 2006, 632 pp.

[14] S.-L. Chung, D. Liu, J. Ji, M.-F. Chu, H.-Y. Lee, D.-J. Wen, C.-H. Lo, T.-Y. Lee, Q. Qian, Q. Zhang, Adakites from continental collision zones: melting of thickened lower crust beneath southern Tibet, Geology 31 (2003) 1021–1024.

[15] Z.-Q. Hou, Y.-F. Gao, X.-M. Qu, Z.-Y. Rui, X.-X. Mo, Origin of adakitic intrusives generated during mid-Miocene east–west extension in southern Tibet, Earth Planet. Sci. Lett. 220 (2004) 139–155.

[16] Q. Wang, F. McDermott, J. Xu, H. Belloon, Y. Zhu, Cenozoic K-rich adakitic volcanic rocks in the Hohxil area, northern Tibet: lower-crustal melting in an intracontinental setting, Geology 33 (2005) 465–468.

[17] W. Deng, H. Sun, Y. Zhang, Age of the Cenozoic volcanic rocks from Nanqian basin, Qinghai Province, Chin. Sci. Bull. 44 (1999) 2554–2558.

[18] F. Roger, P. Tapponnier, N. Arnaud, U. Scharer, M. Brunel, Z. Xu, J. Yang, An Eocene magmatic belt across central Tibet: mantle subduction triggered by the Indian collision? Terra Nova 12 (2000) 102–108.

[19] W.M. Deng, H.J. Sun, Y.Q. Zhang, Petrogenesis of Cenozoic potassic volcanic rocks in Nangqen basin, Chin. J. Geol. 36 (2001) 304–318.

[20] M.S. Spurlin, A. Yin, B.K. Horton, J. Zhou, J. Wang, Structural evolution of the Yushu–Nangqian region and its relationship to syncollisional igneous activity, east-central Tibet, Geol. Soc. Amer. Bull. 117 (2005) 1293–1317.

[21] C. Coulon, H. Maluski, C. Bollinger, S. Wang, Mesozoic and Cenozoic volcanic rocks from central and southern Tibet: ^{39}Ar–^{40}Ar dating, petrological characteristics and geodynamical significance, Earth Planet. Sci. Lett. 79 (1986) 281–302.

[22] J.L.D. Kapp, T.M. Harrison, P. Kapp, M. Grove, O.M. Lovera, L. Ding, The Nyainqentanglha Shan: a window into the tectonic, thermal, and geochemical evolution of the Lhasa block, southern Tibet, J. Geophys. Res. 110 (2005) B08413, doi:10.1029/02004JB003330.

[23] U. Schärer, R.H. Xu, C.J. Allégre, U–Pb geochronology of Gandese (Transhimalaya) plutonism in the Lhasa–Xigaze region Tibet, Earth Planet. Sci. Lett. 69 (1984) 311–320.

[24] C. Miller, R. Schuster, U. Klotzli, W. Frank, B. Grasemann, Late Cretaceous–Tertiary magmatic and tectonic events in the Transhimalaya batholith (Kailas area, SW Tibet), Schweiz. Mineral. Petrogr. Mitt. 80 (2000) 1–20.

[25] X.X. Mo, Z.D. Zhao, J.F. Deng, G.C. Dong, S. Zhou, T.Y. Guo, S.Q. Zhang, L.L. Wang, Response of volcanism to the India–Asia collision, Earth Sci. Front. 10 (2003) 135–148.

[26] P.G. DeCelles, D.M. Robinson, G. Zandt, Implications of shortening in the Himalayan fold–thrust belt for uplift of the Tibetan Plateau, Tectonics 21 (2002) 1062, doi:10.1029/2001TC001322.

[27] G. Maheo, S. Guillot, J. Blichert-Toft, Y. Rolland, A. Pecher, A slab breakoff model for the Neogene thermal evolution of South

Karakorum and South Tibet, Earth Planet. Sci. Lett. 195 (2002) 45–58.
[28] S. Nomade, P.R. Renne, X. Mo, Z. Zhao, S. Zhou, Miocene volcanism in the Lhasa block, Tibet: spatial trends and geodynamic implications, Earth Planet. Sci. Lett. 221 (2004) 227–243.
[29] H.M. Williams, S.P. Turner, J.A. Pearce, S.P. Kelley, N.B.W. Harris, Nature of the source regions for post-collisional, potassic magmatism in southern and northern Tibet from geochemical variations in inverse trace element modeling, J. Petrol. 45 (2004) 555–607.
[30] Z. Guo, M. Wilson, J. Liu, Q. Mao, Post-collisional, potassic and ultrapotassic magmatism of the northern Tibetan plateau: constraints on characteristics of the mantle source, geodynamic setting and uplift mechanisms, J. Petrol. 47 (2006) 1177–1220.
[31] J. Cheng, G. Xu, Geologic map of the Gaize region with report: Chengdu, Tibetan Bureau of Geology and Mineral resources, scale 1:1,000,000 (1987) 369 pp.
[32] P. Kapp, A. Yin, T.M. Harrison, L. Ding, Cretaceous–Tertiary shortening, basin development, and volcanism in central Tibet, Geol. Soc. Amer. Bull. 117 (2005) 865–878.
[33] S. Lai, J. Qin, Y. Li, X. Liu, Cenozoic volcanic rocks in the Belog Co area, Qiangtang, northern Tibet, China: petrochemical evidence for partial melting of the mantle–crust transition zone, Geol. Bull. China 25 (2006) 64–69.
[34] C. Li, X. Huang, S. Mou, X. Chi, Age dating of the Zougouyouchacuo volcanic rocks and age determination of the Kangtog Formation in southern Qiangtang, northern Tibet, Geol. Bull. China 25 (2006) 226–228.
[35] M. Taylor, A. Yin, F.J. Ryerson, P. Kapp, L. Ding, Conjugate strike–slip faulting along the Bangong–Nujiang suture zone accommodates coeval east–west extension and north–south shortening in the interior of the Tibetan Plateau, Tectonics 22 (2003) 1044, doi:10.1029/2001TC001362.
[36] I. McDougall, T.M. Harrison, Geochronology and Thermochronology by the $^{40}Ar/^{39}Ar$ Method, Oxford University Press, New York, 1999, 261 pp.
[37] R.H. Steiger, E. Jäger, Subcommission on geochronology: convention on the use of decay constants in geo- and cosmochronology, Earth Planet. Sci. Lett. 36 (1977) 359–362.
[38] J.-H. Wang, A. Yin, T.M. Harrison, M. Grove, Y.-Q. Zhang, G.-H. Xie, A tectonic model for Cenozoic igneous activities in the eastern Indo–Asian collision zone, Earth Planet. Sci. Lett. (2001) 123–133.
[39] G.T. Brey, T. Köhler, Geothermobarometry in four phase lherzolites, part II. New thermobarometers, and practical assessment of existing thermobarometers, J. Petrol. 31 (1990) 1353–1378.
[40] E. Schmädicke, Phase relations in peridotitic and pyroxenitic rocks in the model systems CMASH and NCMASH, J. Petrol. 41 (2000) 69–86.
[41] B.R. Hacker, G.A. Abers, Subduction Factory 3: An Excel worksheet and macro for calculating the densities, seismic wave speeds, and H_2O contents of minerals and rocks at pressure and temperature, Geochem. Geophys. Geosyst. 5 (2004), Q01005, doi:10.1029/2003GC000614.
[42] N.I. Christensen, Poisson's ratio and crustal seismology, J. Geophys. Res. 101 (1996) 3139–3156.
[43] R. Meissner, F. Tilmann, S. Haines, About the lithospheric structure of central Tibet based on seismic data from the INDEPTH III profile, Tectonophysics 380 (2004) 1–25.
[44] A. Ozacar, G. Zandt, Crustal seismic anisotropy in central Tibet: implications for deformational style and flow in the crust, Geophys. Res. Lett. 31 (2004) L23601, doi:10.1029/22004GL021096.
[45] M.P. Coward, W.S.F. Kidd, Y. Pan, R.M. Shackleton, H. Zhang, The structure of the 1985 Tibet Geotraverse, Lhasa to Golmud, Philos. Trans. R. Soc. Lond. Ser. A: Math. Phys. Sci. 327 (1988) 307–336.
[46] A. Yin, T.M. Harrison, Geologic evolution of the Himalayan–Tibetan orogen, Annu. Rev. Earth Planet. Sci. 28 (2000) 211–280.
[47] P. Kapp, A. Yin, C.E. Manning, M. Murphy, T.M. Harrison, M. Spurlin, L. Ding, X.-G. Deng, C.-M. Wu, Blueschist-bearing metamorphic core complexes in the Qiangtang block reveal deep crustal structure of northern Tibet, Geology 28 (2000) 19–22.
[48] P. Kapp, A. Yin, C.E. Manning, T.M. Harrison, M.H. Taylor, L. Ding, Tectonic evolution of the early Mesozoic blueschist-bearing Qiangtang metamorphic belt, central Tibet, Tectonics 22 (2003) 1043, doi:10.1029/2002TC001383.
[49] W. Zhao, J. Mechie, L.D. Brown, J. Guo, S. Haines, T. Hearn, S.L. Klemperer, Y.S. Ma, R. Meissner, K.D. Nelson, J.F. Ni, P. Pananont, R. Rapine, A. Ross, J. Saul, Crustal structure of central Tibet as derived from project INDEPTH wide-angle seismic data, Geophys. J. Int. 145 (2001) 486–498.
[50] A. Galve, M. Jiang, A. Hirn, M. Sapin, M. Laigle, B. De Voogd, J. Gallart, H. Qian, Explosion seismic P and S velocity and attenuation constraints on the lower crust of the North-Central Tibetan Plateau, and comparison with the Tethyan Himalayas: implications on composition, mineralogy, temperature, and tectonic evolution, Tectonophysics 412 (2006) 141–157.
[51] P. Kapp, M.A. Murphy, A. Yin, T.M. Harrison, L. Ding, J. Guo, Mesozoic and Cenozoic tectonic evolution of the Shiquanhe area of western Tibet, Tectonics 22 (2003) 1029, doi:10.1029/2001TC001332.
[52] J.H. Guynn, P. Kapp, A. Pullen, M. Heizler, G. Gehrels, L. Ding, Tibetan basement rocks near Amdo reveal "missing" Mesozoic tectonism along the Bangong suture, central Tibet, Geology 34 (2006) 505–508.
[53] M.N. Ducea, V. Lutkov, V.T. Minaev, B. Hacker, L. Ratschbacher, P. Luffi, M. Schwab, G.E. Gehrels, M. McWilliams, J. Vervoort, J. Metcalf, Building the Pamirs: the view from the underside, Geology 31 (2003) 849–852.
[54] P. Tapponnier, Z. Xu, F. Roger, B. Meyer, N. Arnaud, G. Wittlinger, J. Yang, Oblique stepwise rise and growth of the Tibet Plateau, Science 294 (2001) 1671–1677.